3

Design and Validation of a Universal 6D Seam Tracking System in Robotic Welding Based on Laser Scanning

Mikael Fridenfalk, Gunnar Bolmsjö
Lund University
Sweden

1. Introduction

Robot automation increases productivity, the product quality and frees man from involuntary, unhealthy and dangerous work. While computational power has increased exponentially during the last decades, the limitations in flexibility constitute today a bottleneck in the further evolution of robotic systems.

One application for intelligent systems is seam tracking in robotic welding. Seam tracking is among others used for the manufacturing of large ships such as cruisers and oil tankers, where relatively high tolerances in the sheet material are allowed to minimize the manufacturing costs (Bolmsjö, 1997; Fridenfalk & Bolmsjö, 2002a). Seam tracking is today typically only performed in 2D, by a constant motion in x and compensation of the errors in y and z directions, see Fig. 1. There exist solutions for higher autonomy that include seam tracking in 3D where compensation is also performed in *o* direction or around an orientation axis. These limitations make however seam tracking only possible for work pieces with relatively simple geometrical shapes.

The next step in the evolution of sensor systems in robotic welding is the introduction of a full 6D sensor guided control system for seam tracking which is able to correct the TCP in x, y, z and around roll, pitch and yaw. Such an ultimate system is per definition able to follow any continuous 3D seam with moderate curvature. This system has many similarities with an airplane control system, where a change in either position or orientation affects all other degrees of freedom.

Though seam tracking has been performed in 2D for at least 40 years, the hypothetical design of 6D seam tracking systems was probably first addressed in the beginning of the last decade by suggestions of models based on force sensors (Bruyninckx et al.,1991a; Bruyninckx et al., 1991b) and laser scanners (Nayak & Ray, 1990a; Nayak & Ray, 1990b). It is however difficult to evaluate these systems, since no experimental results are presented, neither any explicit control systems for creating balance between the subsystems.

The contribution of this paper is the invention of a universal 6D seam tracking system for robotic welding, validated by simulation experiments based on physical experiments, which proved that 6D seam tracking is possible and even very robust for laser scanning (Fridenfalk & Bolmsjö, 2002b). On a more detailed level, the contributions of this paper are considered to be the introduction of: (1) differential control in laser scanning, using the same techniques

Source: Industrial Robotics: Programming, Simulation and Applicationl, ISBN 3-86611-286-6, pp. 702, ARS/plV, Germany, December 2006, Edited by: Low Kin Huat

as used in arc sensing (Cook et al., 1987), (2) trajectory tangent vector control using differential vector interpolation, and (3) pitch control by vector interpolation. These components constitute the foundation of the 6D seam tracking system.

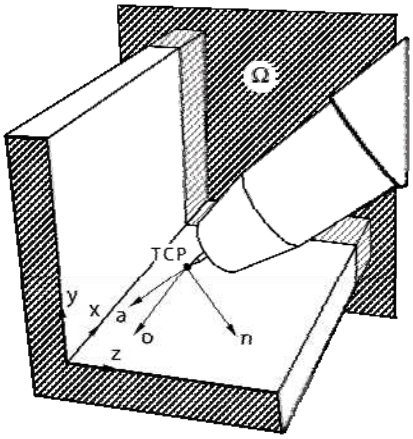

Fig. 1. Definition of Tool Center Point (TCP) and the orthonormal coordinate system {*n, o, a*}. Here, *o* is opposite to the direction of welding and perpendicular to the plane Ω, and *a* is the direction of approach. {x, y, z} is a local coordinate system, defined for the work-piece.

The authors have found only a few references from the literature which describe similar work, which is the introduction of a trajectory tangent vector by curve fitting (Nayak & Ray, 1990a; Nayak & Ray, 1990b). There exist however some essential differences between how such trajectory vector was used and implemented. The differences consist of (1) curve fitting by 2nd instead of 3rd degree polynomials, for faster computation and still high control stability, (2) using an analytic solver for curve fitting of 2nd degree polynomials developed and implemented for this system, increasing the calculation speed further and (3) using differential vector interpolation instead of direct use of the trajectory tangent vector, which showed to be essential for maintaining control stability.

The accuracy needed to perform robotic arc welding depends on the welding process. In our case we were working with GMAW (Gas Metal Arc Welding). The accuracy needed to follow the seam and position the weld torch relative the weld joint is in the order of ± half diameter of the welding wire, or ±0.6 mm in our case. As indicated above and shown in our simulations, the curvature or radius is an important measure of the performance of the system. As shown from simulation experiments, seam tracking curves with a radius down to 20 mm produces no added positional error during continuous path motion in the sensor feed-back loop which controls the robot. However, the torch angle changes from a 4 degrees deviation at 50 mm radius to 12 degrees at 20 mm radius. Thus, the accuracy needed for this process can be obtained by the system provided the sensor and robot have matching specifications. As indicated by the results, the system can be used for welding processes which requires higher accuracy providing the robot and sensor can meet this as well.

A 6D seam tracking system increases the capability and flexibility in manufacturing systems based on robotic welding using laser scanning. This reduces the need for accurate robot trajectory programming and geometrical databases. The simulation results (based on physical experiments) showed that the initial objective to design a 6D seam tracking system

was reached that could manage a radius of curvature down to 200 mm. Furthermore, if low-speed seam tracking is performed without welding, to find the geometry of the work-piece, there is basically no limit how small radius of curvature this system is able to manage.

2. Materials and methods

2.1 Sensors guided robot control

Many systems have been developed during the last decades for seam tracking at arc welding. The patents and scientific publications within this application area show that laser scanners and arc sensors today replace older systems. Laser scanners have in general high accuracy but are expensive and have to be mounted on the torch, thereby decreasing the workspace of the robot. This problem is partly solved by introduction of an additional motion that rotates the scanner around the torch to keep its relative orientation constant with respect to the seam profile. In practical applications presently, solutions based on pure image processing by a CCD camera are further successfully used to find the initial point where the seam tracking should start (Fridenfalk & Bolmsjö, 2002a), in addition to the laser scanner sensor.

2.1.1 Laser scanning

In laser scanning, the seam profile is extracted by periodically scanning the laser beam across a plane perpendicular to the direction of the seam. The laser scanner is mounted on the torch in front of the direction of welding. As a general rule, the control system is based on full compensation of the position errors, which is equal to a constant value of $K_1 = 1$, as defined in Fig. 2.

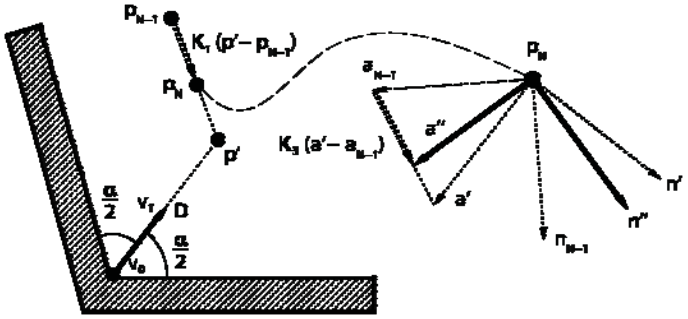

Fig. 2. Cross section, plane Ω. Vector interpolation used for position and pitch control at laser scanning. The input from the laser scanner system is the intersection point of the seam walls v_0 and the unit vector v_1 on Ω between the seam walls. D denotes the distance between v_0 and p'.

2.1.2 Arc sensing

Another method used for seam tracking is "through-arc" sensing or simply arc sensing (Cook et al., 1987). Here, the arc current is sampled while a weaving motion is added to the TCP in n direction, see Fig. 1. Since the distance from TCP to the nearest seam wall may be approximately calculated as a function of the current, it is possible to compensate for deviations in the seam by analysis of the current measurements. Arc sensors are inexpensive, do not decrease the workspace of the robot, but are compared with other sensors for seam tracking relatively inaccurate due to the stochastic nature of arc welding. Since welding of large structures in

general requires a relatively low accuracy however, arc sensors are a competitive alternative to laser scanners. Arc sensing may also be used as a complementary sensor to laser scanners in some cases where the laser scanner is unable to access the seam track.

2.1.3 Virtual sensors

The development of sensor guided control systems may be accelerated using virtual sensors in the simulation control loop. Since a system's state is often easily obtained in simulation, assuming that the simulation model is sufficiently accurate compared to the real system, this provides for a better foundation for process analysis than in general is possible by physical experiments. Furthermore, insertion of a sensor in a control loop may cause damage to expensive equipment, unless the behaviour of the entire sensor guided control system is precisely known, which is rarely the case at the development stage. Virtual sensors are used in many application areas, such as robotics, aerospace and marine technologies (Bolmsjö, 1999; Dogget & Vazquez, 2000; Hailu & Zygmont, 2001; Oosterom & Babuska, 2000; Ridao et al., 2001). Development of new robot systems such as for seam tracking may be accelerated by the use of simulation (Fridenfalk et al., 1999a; Fridenfalk et al., 1999b). In the development of virtual sensors, if the model is not analytically definable, artificial neural networks or statistical methods are often used (Arroyon et al., 1999; Pasika et al., 1999).

2.2 Robot system

The design of the 6D seam tracking system was based on experiments and results from the European ROWER-2 project (European Commission, 2002). The objective of this project was to automate the welding process in shipbuilding by the design of a robotic system, specifically for joining double-hull sections in super-cruisers and oil tankers. Figure 3 shows the robot system developed in the ROWER-2 project and the corresponding simulation model in FUSE (described below). The implementation of the 3D seam tracking system was performed in C/C++, running on a QNX-based embedded controller (QNX is a real-time operating system for embedded controllers). The robot was manufactured partly in aluminium alloy to decrease the weight for easy transportation and mounted on a mobile platform with 1 degree of freedom for increased workspace. The robot system was integrated and successfully validated on-site at a shipyard.

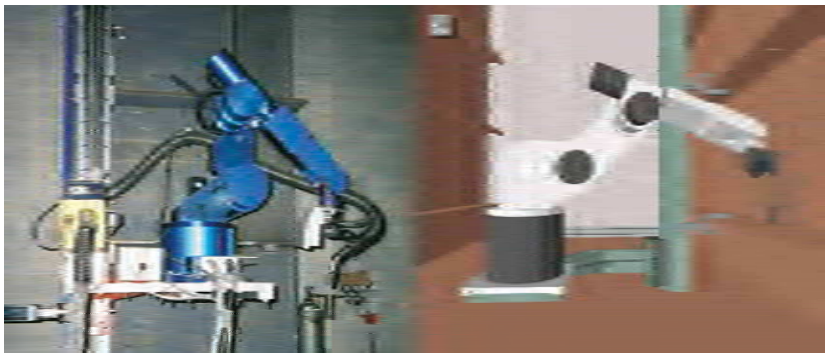

Fig. 3. The design of the robot system for 3D seam tracking based on arc sensing in the ROWER-2 project (left) was based on simulations in FUSE (right). The 6D seam tracking system presented here was developed based on experience and results gained from the ROWER-2 project.

2.3 Simulation system

The development and implementation of the 6D seam tracking system was initially performed in the Flexible Unified Simulation Environment (FUSE) (Fridenfalk & Bolmsjö, 2001). FUSE is an integrated software system based on Envision (robot simulator, Delmia Inc.) and Matlab (MathWorks Inc.), including Matlab Robot Toolbox (Corke, 1996). The integration was performed by compiling these software applications and their libraries into one single software application, running under IRIX, SGI. The methodology developed for the design of the 6D seam tracking system was based on the integration of mechanical virtual prototyping and software prototyping. The 6D seam tracking simulations in FUSE were performed by using the robot developed in the ROWER-2 project and an ABB S4 IRB2400.16 robot, see Figs. 3 and 4. After the design and successful validation of a 6D seam tracking system for arc sensing, the virtual prototyping and software models, partly written in C-code and partly in Matlab code, were translated to pure Matlab code. The Matlab models were modified to work also for laser scanners by the addition of a virtual model of the Servo-Robot M-SPOT laser scanner system. The translation was necessary, since it saved development time for the implementation of the evaluation system, for the accurate calculation of position and orientation errors during simulation.

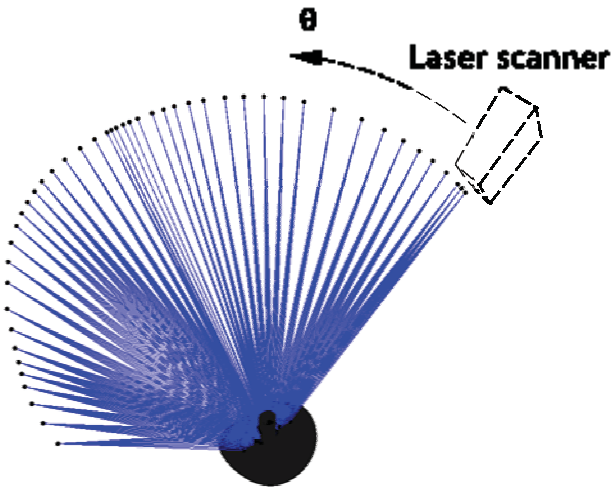

Fig. 4. Example of a 6D seam tracking experiment performed in Matlab. Each laser scan is plotted at each control cycle while seam tracking is performed 180° around a pipe intersection. The work-piece object corresponds to the object in the upper experiment in Fig. 7.

2.4 Calculation of position and orientation errors

Error is defined as the difference between desired and current pose **P**. The position errors were calculated by projection of ε_a and ε_n on a plane Ω_t perpendicular to the desired trajectory while intersecting current TCP, $\mathbf{P}_t$. Thereby, per definition $\varepsilon_o = 0$. The orientation error (the orientation part of $\mathbf{P}_\delta$) is calculated by:

$$\mathbf{P}_\delta = \mathbf{P}_t^{-1} \cdot \mathbf{P}_{\Omega_t} \tag{1}$$

where $\mathbf{P}_t$ is the current TCP and $\mathbf{P}_{\Omega t}$ is the desired TCP for any sample point t. The errors around n, o and a were calculated by the subsequent conversion of the resulting transformation matrix to roll, pitch and yaw, here defined as rotation around, in turn, a, o and n. Rotation in the positive direction is defined as counter clockwise rotation from the perspective of a viewer when the axis points towards the viewer.

3. Modelling

In this section the design of the 6D seam tracking system is described. The principal control scheme of this system is presented in Fig. 5. The control system is based on three main components, position, trajectory tangent vector and pitch control. Pitch denotes rotation around o. The main input of this control system is the 4×4 transformation matrix $\mathbf{P}_{N-1}$, denoting current TCP position and orientation. The output is next TCP, $\mathbf{P}_N$. N is the number of samples used for orientation control. The input parameters are N, the proportional control constants K_1, K_2 and K_3, and the generic sensor input values $\xi = [v_0\ v_1]$ and $\zeta = v_1$, where v_0 and v_1 are defined in Fig. 2. The proportional constants K_1, K_2 and K_3 denote the control response to errors in position, trajectory tangent vector and pitch control. N is also used in trajectory tangent vector control and is a measure of the memory size of the algorithm. The seam profile presented in Fig. 1 is a fillet joint. Since v_0 and v_1 may be extracted for any joint with a predefined signature, no other joints were required in the experiments.

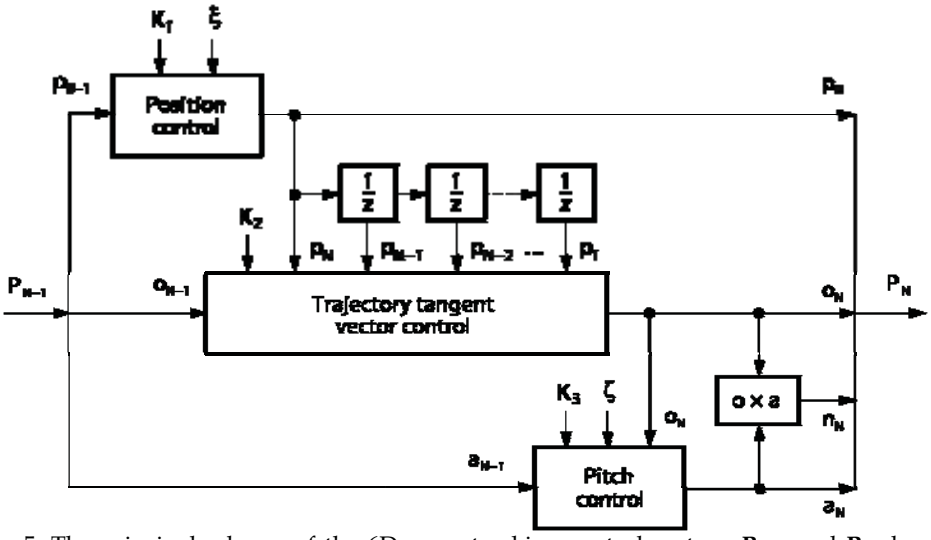

Fig. 5. The principal scheme of the 6D seam tracking control system. $\mathbf{P}_{N-1}$ and $\mathbf{P}_N$ denote current and next TCP. $\mathbf{P}_N$ is calculated for each control sample designated for the seam tracking motion.

3.1 Position control

The 6D seam tracking algorithm starts by the calculation of next position for the TCP. Next position p_N is calculated by vector interpolation based on K_1 in Fig. 2, between current position p_{N-1} and the position p´ extracted from the laser scanner.

3.2 Trajectory tangent vector control

The positions $p_1 ... p_N$ are used for trajectory estimation by curve fitting, see Fig. 6. To decrease calculation time, an analytical estimator was devised for 1st and 2nd degree polynomials that showed to work much faster than traditional matrix multiplication followed by inversion techniques using Gauss elimination. The estimation of the trajectory at N gives o'. Since an attempt to abruptly change the direction of o from o_{N-1} to o' would most probably create instability in the system, the motion between o_{N-1} and o' is balanced by vector interpolation using K_2. The scalar κ_2 is not explicitly used in the calculations, but used for visualization of the calculation of o_N in Fig. 6.

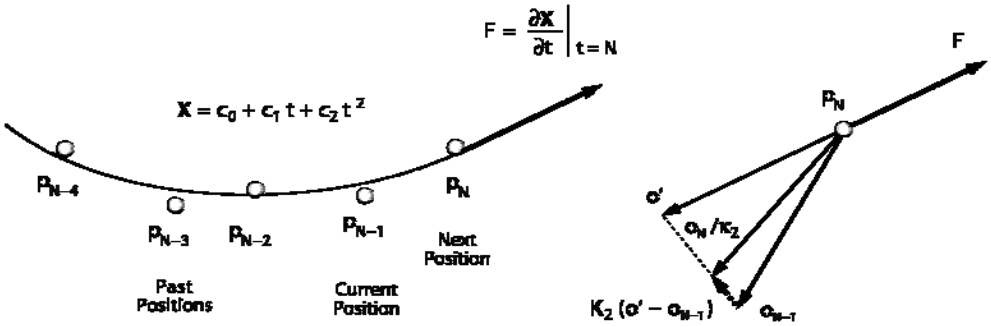

Fig. 6. Trajectory tangent vector control is performed by the least square curve fitting of the last N trajectory points (left) to a 2nd degree polynomial curve for x, y and z, followed by vector interpolation (right). Here N = 5. X, c_0, c_1 and c_2 denote vector entities. The trajectory tangent vector F is for a 2nd degree polynomial equal to $c_1 + 2Nc_2$.

3.3 Pitch control

The first step in pitch control is performed by vector interpolation between a_{N-1} and a', using K_3, see Fig. 2. In a second step, a_N is calculated by orthogonally projecting a'' on a plane perpendicular to o_N and normalization of the resulting vector. Finally, n_N is calculated by the cross product $o_N \times a_N$.

3.4 Code and pseudo code samples

The actual implementation of the 6D seam tracking system showed to be straightforward. Most of the development effort was spent on the design of the surrounding environment of the seam tracking system, including a semi-automatic testing and evaluation system. In simulation, the plane Ω is assumed to intersect the TCP point. In reality however, the laser scanner is mounted on the torch, often several centimetres ahead of the direction of the motion. The transformation to such system at real-time control is performed by storing the trajectory data for use with a time delay. A pseudo code representation of the 6D seam tracking system in Fig. 5, follows below:

1. $p_N = p_{N-1} - r_w \cdot o_{N-1} + K_1 \cdot (v_0 + D \cdot v_1 - p_{N-1})$, where v_0, v_1 and D are defined in Fig. 2 and r_w is the nominal displacement in the direction of welding during a control sample.
2. Calculation of x_N by shifting x_{N-1} one step to the left with p_N: $x_{N-1} = [p_0\ p_1\ ...\ p_{N-2}\ p_{N-1}] \rightarrow x_N = [p_1\ p_2\ ...\ p_{N-1}\ p_N]$.
3. Estimation of the trajectory tangent vector F by least square curve fitting of the parameterized 3D curve $X = C \cdot T$ with a parameter t to 3 independent second-degree

polynomials (for x, y and z). $F = \partial X/\partial t\,|_{t=N}$ with $X = C \cdot T$, where $C = [c_0\ c_1\ c_2] = [c_x\ c_y\ c_z]^T$ and $T = [1\ t\ t^2]^T$ (Note that A^T is the transpose function for a vector or matrix A and has no correlation with the vector T). This gives $F = C \cdot \partial T/\partial t\,|_{t=N} = C \cdot [0\ 1\ 2t]^T\,|_{t=N} = C \cdot [0\ 1\ 2N]^T$. C is calculated by the estimation of the parameters c_i for i = {x, y, z}, where $c_i = (A^TA)^{-1}(A^Tp_i)$ and p_i are the row vectors of x_N, which may also be written as $x_N = [p_x\ p_y\ p_z]^T$. The matrix A consists of N rows of $[1\ t\ t^2]$ with t = 1...N, where t is the row number. It should be mentioned that C may be directly calculated by the expression $C = ((A^TA)^{-1}(A^T\ x_N{}^T))^T$, but we have chosen to use the notation above for pedagogical reasons.

4. $o_N = \text{normalize}(o_{N-1} - K_2 \cdot (\text{normalize}(F) + o_{N-1}))$. Normalization of a vector v denotes v divided by its length.
5. $a'' = a_{N-1} - K_3 \cdot (a_{N-1} + v_1)$.
6. $a_N = \text{normalize}(a'' - \text{dot}(o_N, a') \cdot o_N)$, where dot (o_N, a') is the dot product $o_N{}^T \cdot a''$.
7. $\mathbf{P}_N = \begin{bmatrix} o_N \times a_N & o_N & a_N & p_N \\ 0 & 0 & 0 & 1 \end{bmatrix}$

The initial value of x is determined by linear extrapolation with respect to the estimated direction at the beginning of the seam. The elements of F(i) with i = {1, 2, 3} for {x, y, z} were here calculated by the Matlab function pfit((1:N)',x(i,:)') (the input parameters x and y in this function are $[1\ 2\ ...\ N]^T$ and b_i as defined above). The pfit function was developed in this work using Maple (Waterloo Maple Inc.) and gives an analytical solution to 2nd degree polynomial curve fitting for this application, that showed to work 8 times faster for N = 10 and 4 times faster for N = 100 than the standard Matlab function polyfit. The analytical function pfit was implemented according to below:

```
function k = pfit(x,y)
  n = length(x); sx = sum(x); sy = sum(y); sxx = x'*x; sxy = x'*y;
  sx3 = sum(x.^3); sx4 = sum(x.^4); sxxy = sum(x.^2.*y);
  t2 = sx*sx; t7 = sx3*sx3; t9 = sx3*sxx; t12 = sxx*sxx;
  den = 1/(sx4*sxx*n-sx4*t2-t7*n+2.0*t9*sx-t12*sxx);
  t21 = (sx3*n-sxx*sx)*t15;
  k = 2.0*n*((sxx*n-t2)*t15*sxxy-t21*sxy+(sx3*sx-t12)*t15*sy)- ...
  t21*sxxy+(sx4*n-t12)*t15*sxy+(t9-sx4*sx)*t15*sy;
```

The calculation speed was optimization by the application of Cramer's rule by an analytical inversion of A^TA in Maple and the elimination of c_0. In the function above, x and y are N × 1 column vectors, x´ equals x^T, sum(x) is the sum of the vector elements of x, and a point before an operator such as the exponential operator ^, denotes element-wise operation. This implementation may be further optimized by reusing terms that only depend on x in pfit (which is equal to t outside pfit). Since such optimization is however outside the scope of this paper, we have chosen to keep this presentation as simple as possible.

3.5 Computational costs

The computational costs for the 6D seam tracking system based on laser scanning (without consideration to memory operations or index incrementation) was preliminary estimated to less than 250 + 50N floating point operations for the implementation presented in this paper, which for N = 10 gives 750 operations per control cycle. At a rate of maximum 30 scans per second, this gives less than 22.500 floating point operations per second.

3.6 Kinematics singularities

In sensor guided control, the manipulator may involuntarily move into areas in which no inverse kinematics solutions exist, generally called kinematics singularities. It is however possible to minimize inner singularity problems caused by robotic wrists. A novel method is suggested in (Fridenfalk, 2002) which was designed for the 6D seam tracking system, but works basically for any industrial robot with 6 degrees of freedom. In this method, the stronger motors, often at the base of the robot, assist the weaker wrist motors to compensate for any position error. This method allows also for smooth transitions between different configurations. In addition to this, in one-off production or for generation of a reference program, pre-scanning and trial run may be performed before welding. In the first step, low-speed (or high-speed) seam tracking is performed to calculate the trajectory of the TCP, following the seam. In the second step, a trial run is performed in full speed to check the performance of the robot, and finally the actual welding is performed.

3.7 Initial and final conditions

In the experiments, seam tracking was initiated from a proper position already from start. The start position for seam tracking is in general found either by image analysis using a camera or by seam tracking itself. Since previous positions are unknown at start, estimation is made of previous $N-1$ positions, by extrapolation of the trajectory in the direction of o. This is the reason why in some experiments, higher orientation errors occurred at the beginning of seam tracking. The condition to stop seam tracking may be based on the position of the TCP. The stop signal may be triggered by definition of volumes outside which no seam tracking is allowed.

4. Experimental results

4.1 Work-piece samples

The position and orientation errors at seam tracking were calculated based on simulation experiments of basically 8 different work-pieces, see Figs. 7-11. It should be mentioned that the experiments in the bottom of Fig. 8 and Fig. 9 are not actually possible in practice due to collision problems, but are performed for the analysis of the control system. The work-pieces in Matlab were approximated by lines orthogonal to the direction of the weld and the resolution was defined as the nominal distance between these lines. The resolution was here set to 0.02 mm. The reason why no noise was added to the profile obtained from the laser scanner (except for perhaps decreasing the number of measurement points compared to the M-SPOT, which may use up to 512 points per scan), was because large number of measurements allow for high-precision estimations of v_0 and v_1, with a constant offset error less than the accuracy of the laser scanner. Since the 6D seam tracking system corrects the position and the orientation of the TCP relative to the extracted profile, such error will not influence the behaviour of the control system more than highly marginally, by basically adding a small offset error to the experimental results in Figs. 7-11. The work-pieces are categorized into two groups, continuous and discrete. In the experiments presented in this paper, the range was $0-180^o$ for continuous and 12 mm for discrete work-pieces. In seam tracking of a continuous work-piece, sudden changes is interpreted as a curve with a small radius of curvature, see Figs. 7-8, while in seam tracking of a discrete work-piece a sudden change is regarded as a disturbance, see Figs. 10-11. The settings of the control parameters decide alone the mode of the control system: continuous or discrete. For seam tracking of objects with a large radius of curvature, the discrete mode works well for both continuous and discrete work-pieces, see Fig. 9.

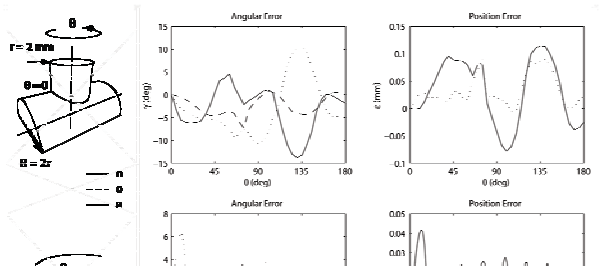
r= 2 mm
H = 2r
Angular Error
Position Error
θ (deg)
γ (deg)
e (mm)
Angular Error
Position Error

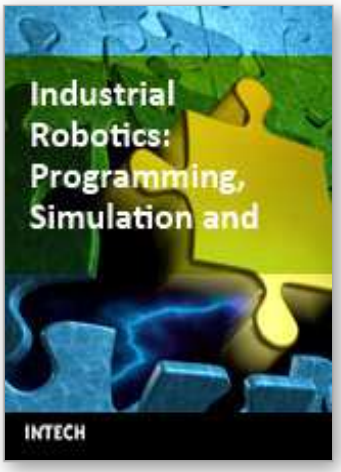

Industrial Robotics: Programming, Simulation and Applications

Edited by Low Kin Huat

ISBN 3-86611-286-6

Hard cover, 702 pages

Publisher Pro Literatur Verlag, Germany / ARS, Austria

Published online 01, December, 2006

Published in print edition December, 2006

This book covers a wide range of topics relating to advanced industrial robotics, sensors and automation technologies. Although being highly technical and complex in nature, the papers presented in this book represent some of the latest cutting edge technologies and advancements in industrial robotics technology. This book covers topics such as networking, properties of manipulators, forward and inverse robot arm kinematics, motion path-planning, machine vision and many other practical topics too numerous to list here. The authors and editor of this book wish to inspire people, especially young ones, to get involved with robotic and mechatronic engineering technology and to develop new and exciting practical applications, perhaps using the ideas and concepts presented herein.

InTech Europe
University Campus STeP Ri
Slavka Krautzeka 83/A
51000 Rijeka, Croatia
Phone: +385 (51) 770 447
Fax: +385 (51) 686 166
www.intechopen.com

InTech China
Unit 405, Office Block, Hotel Equatorial Shanghai
No.65, Yan An Road (West), Shanghai, 200040, China
中国上海市延安西路65号上海国际贵都大饭店办公楼405单元
Phone: +86-21-62489820
Fax: +86-21-62489821